Synthesis, Crystallographic and Spectroscopic Characterization, and Magnetic Properties of Mixed-Ligand Oxovanadium(IV) Hydrotris(3,5-dimethylpyrazolyl)borate Complexes

David Collison,*,† David R. Eardley,† Frank E. Mabbs,† Anne K. Powell,*,‡ and Scott S. Turner†

Department of Chemistry, University of Manchester, Manchester M13 9PL, U.K., and School of Chemical Sciences, University of East Anglia, Norwich NR4 7TJ, U.K.

Received March 11, 1992

The synthesis and crystallographic characterization of three oxovanadium(IV) complexes as solvates are reported: (a) [{HB(Me_2pz)$_3$}VOCl(Me_2pzH)]·2MeCN (I·2MeCN), (b) [{HB(Me_2pz)$_3$}VO(benzoate)(Me_2pzH)]·0.4toluene (II·0.4toluene), and (c) [{HB(Me_2pz)$_3$}VO(μ-malonate)VO(Me_2pzH){HB(Me_2pz)$_3$}]·2toluene (III.2toluene), where Me_2pz = 3,5-dimethylpyrazolyl. I·2MeCN: blue rhombs; triclinic, $P\bar{1}$; a = 9.986(3), b = 10.898(3), c = 16.007(3) Å; α = 71.50(2), β = 79.86(2), γ = 65.70(2)°; Z = 2. II·0.4toluene: purple hexagonal prisms; trigonal $P\bar{3}$; a = 24.320(3), c = 9.233(1) Å; Z = 6. III·2toluene: purple/blue rhombs; triclinic $P\bar{1}$; a = 13.859(4), b = 13.843(3), c = 16.860(4) Å; α = 76.07(2), β = 72.50(2), γ = 73.77(2); Z = 2. In each case the metal is found in a distorted octahedral environment with a short vanadium to terminal oxygen distance: (I) 1.599(4), (II) 1.590(8), (III) 1.587(9), 1.592(9) Å. The hydrotris(3,5-dimethylpyrazolyl)borate ion acts as a facially coordinating, uninegative tridentate ligand, and in each case one neutral pyrazole molecule is used to complete six-coordination at the metal. In II the benzoate anion acts as a monodentate ligand, and in III the malonate anion is monodentate with respect to one vanadium center and bridges to the other, forming a six-membered chelate ring system, such that one carboxylate functionality forms the bridge unit. The neutral pyrazole molecule is held in the same relative position by hydrogen bonding in complexes II and III but has a different orientation with respect to the LVO fragment in I. The three complexes have been characterized by infrared, electronic absorption and ESR spectroscopy and by cyclic voltammetry at a platinum working electrode. The ESR spectra recorded in dichloromethane solution are consistent with a monomer structure for I and II and with the retention of a dimer for III. Double-integrated ESR signal intensities measured in the temperature range 300–3.6 K for II and III in CH_2Cl_2 solution show an antiferromagnetic coupling interaction in III of ca. 3 cm^{-1}.

Introduction

There is currently much interest[1] in understanding magnetic interactions in coordination complexes for the purposes of designing molecular scale devices. In this area Kahn[2] has concentrated on the "irregular spin state" approach, while Miller and others[3] have had some success using organometallic and organic compounds. Gatteschi[4] has used metal complexes to which have been attached paramagnetic nitro compounds. We are studying the means by which unpaired electron density is transmitted between paramagnetic centers causing magnetic interactions in a cooperative manner. As an extension of our current work[5] on the magnetic behavior of compounds containing the {LMo(NO)} moiety, we are investigating how the {LVO} unit can form such magnetic interactions. Previously[6] we have studied weak extended exchange interactions between monomeric $[VO]^{2+}$ units in the solid state, notably by single-crystal ESR spectroscopy, where the magnitude of the exchange interaction is comparable to the metal hyperfine splitting. Computer simulation of spectra and variable-temperature measurements were needed to obtain the energy of magnetic exchange interaction of ca. 10^{-1} cm^{-1}.

The use of the sterically-demanding hydrotris(3,5-dimethylpyrazolyl)borate ligand (=L) enables us to study isolated vanadyl centers. Also using this ligand to help control the substitution at the metal enables us to tailor the extent of oligomerization when polyfunctional ligands are introduced into the coordination environment. We have selected carboxylates as the bridging moieties because of their structural flexibility and potential variety in mode of bridging. The way in which carboxylates bind to metals has been the subject of a detailed study by Glusker et al.[7]

The complexes reported here are also relevant to the presence of vanadium in biological systems. Vanadium-containing bromoperoxidases (BPO)[8] catalyze the peroxide-dependent halogenation of organic substrates in marine algae, notably *Ascophyllum nodosum*. Although it is the 5+ oxidation state rather than the 4+ which is physiologically active, the latter state can be generated by dithionite reduction and is very useful for spectroscopic studies.[9] EXAFS measurements[10a] show that in both oxidation states there is at least one short, terminal vanadium–oxygen bond, with additional light-atom (O,N) coordination.

† University of Manchester.
‡ University of East Anglia.

(1) *Magnetic Molecular Materials*; Gatteschi, D., Kahn, O., Miller, J. S., Palacio, F., Eds.; Kluwer: Dordrecht, The Netherlands, 1991.
(2) (a) Kahn, O. *Struct. Bonding* **1987**, *68*, 69. (b) Nakatani, K.; Carriat, J. Y.; Journaux, Y.; Kahn, O.; Lloret, F.; Renard, J. P.; Pei, Y.; Sletten, J.; Verdaguer, M. *J. Am. Chem. Soc.* **1989**, *111*, 5739.
(3) Miller, J. S.; Calabrese, J. C.; Rommelmann, H.; Chittipeddi, S. R.; Zhang, J. H.; Reiff, W. M.; Epstein, A. J. *J. Am. Chem. Soc.* **1988**, *110*, 782.
(4) Caneschi, A.; Gatteschi, D.; Renard, J. P.; Rey, P.; Sessoli, R. *Inorg. Chem.* **1989**, *28*, 2940.
(5) McWhinnie, S. L. W.; Jones, C. J.; McCleverty, J. A.; Collison, D.; Mabbs, F. E. *J. Chem. Soc., Chem. Commun.* **1990**, 940.
(6) Collison, D.; Gahan, B.; Mabbs, F. E. *J. Chem. Soc., Dalton Trans.* **1983**, 1705.
(7) Carrell, C. J.; Carrell, H. L.; Erlebacher, J.; Glusker, J. P. *J. Am. Chem. Soc.* **1988**, *110*, 8651.
(8) See for example: (a) Wever, R.; Tromp, M. G. M. *J. Inorg. Biochem.* **1991**, *43*, 404. (b) Butler, A.; Soedjak, H. S.; Tschirret-Guth, R. A. *J. Inorg. Biochem.* **1991**, *43*, 405. (c) Wever, R.; Kustin, K. *Adv. Inorg. Chem.* **1990**, *35*, 81.
(9) (a) de Boer, E.; Wever, R. *J. Biol. Chem.* **1988**, *263*, 12326. (b) de Boer, E.; Boon, K.; Wever, R. *Biochemistry* **1988**, *27*, 1629.
(10) (a) Arber, J. M.; de Boer, E.; Garner, C. D.; Hasnain, S. S.; Wever, R. *Biochemistry* **1989**, *28*, 7968. (b) de Boer, E.; Keijzers, C. P.; Klaassen, A. A. K.; Reijerse, E. J.; Collison, D.; Garner, C. D.; Wever, R. *FEBS Lett.* **1988**, *235*, 93.

0020-1669/93/1332-0664$04.00/0

ESEEM measurements[10b] have confirmed the presence of nitrogen atoms in the coordination sphere of the enzyme, implying coordination by histidine residues. Carrano et al.[11] have been using the hydrotris(3,5-dimethylpyrazolyl)borate ligand as a model for the imidazole coordination to vanadium. So far, carboxylate oxygen has not been ruled out as a possible ligand for vanadium in BPO (i.e. aspartate, glutamate). Carboxylate ligation to vanadium in the presence of histidine is also thought to be important for vanadium-containing nitrogenase.[12]

Experimental Section

Materials. Unless otherwise stated, reactions were carried out under an atmosphere of dinitrogen using standard Schlenk tube techniques. Solvents were dried and distilled prior to use. Potassium hydrotris(3,5-dimethylpyrazolyl)borate (KL) was prepared as described previously.[13a] The purity of the ligand was confirmed by elemental analysis and infrared and 300-MHz ^{1}H NMR spectroscopy, and the ligand was shown to be free of excess 3,5-dimethylpyrazole. $[VOCl_2(MeCN)_2(H_2O)]$ was prepared as described previously.[13b] Vanadium pentoxide and potassium borohydride (Aldrich), thionyl chloride, silver benzoate and sodium malonate (BDH), and 3,5-dimethylpyrazole (Fluka) were used as received without further purification.

Syntheses. [{HB(Me$_2$pz)$_3$}VOCl(Me$_2$pzH)]·2MeCN (I·2MeCN). $[VOCl_2(MeCN)_2(H_2O)]$ (2.50 g, 10.5 mmol) was dissolved in 100 cm^3 of dry, distilled MeCN to give a clear, blue solution. The solution was stirred and heated to ca. 50 °C, and K{HB(Me$_2$pz)$_3$} (3.10 g, 10.4 mmol) was added to yield a gray precipitate in a blue solution. Stirring was continued at ca. 50 °C for 1 h. The gray solid was removed by centrifugation, and the supernatant was left in a freezer at ca. −30 °C for 2 days to yield a mixture of blue and white solids in a blue/green solution. The solids were collected by filtration and then treated with dichloromethane to dissolve the blue product only. The solution was then evaporated to dryness in vacuo to form a blue solid. Crystallization from MeCN at ca. −30 °C led to a mixture of diamond-shaped and hexagonal blue plates containing two molecules of methyl cyanide per vanadium atom. The crystals lose the solvent of crystallization if left in air and become opaque. In a typical reaction the yield of (I·2MeCN is 20–30% based on vanadium. Anal. Calcd for $C_{24}H_{36}N_{10}BClOV$ (I·2MeCN): C, 49.9; H, 6.24; N, 24.3; V, 8.83. Found: C, 50.1; H, 6.20; N, 24.3; V, 8.90.

[{HB(Me$_2$pz)$_3$}VO(benzoate)(Me$_2$pzH)]·0.4toluene (II·0.4toluene). I·2MeCN (0.135 g, 0.240 mmol) was dissolved in dichloromethane (10 cm^3) to give a clear blue solution. Silver benzoate (0.055 g, 0.240 mmol) was added, and after 5 min of stirring at ambient temperature, a pale gray solid (AgCl) in a purple solution formed. The mixture was left to stir for a period of 30 min, during which time there was no further visible change. The solid was removed by filtration and the filtrate evaporated in vacuo to yield a lilac powder. Crystallization from dichloromethane/toluene (1/1 v/v) gave deep-purple prisms of hexagonal cross section. The yield was 60% based on vanadium. Anal. Calcd for $C_{29.8}H_{38.2}N_8BO_3V$ (II·0.4toluene): C, 57.9; H, 6.23; N, 18.12; V, 8.24. Found: C, 57.9; H, 6.5; N, 18.15; V, 8.4.

[{HB(Me$_2$pz)$_3$}VO(μ-malonate)VO(Me$_2$pzH){HB(Me$_2$pz)$_3$}]·2toluene (III·2toluene). I·2MeCN (0.15 g, 0.26 mmol) was dissolved in MeCN (20 cm^3) to give a clear, blue solution, and sodium malonate (0.019 g, 0.130 mmol) was dissolved in water. The two solutions were mixed with stirring at ambient temperature. After 2 min the resulting solution became purple, and stirring was continued for a further 30 min. The solvent was evaporated in vacuo to give a lilac powder. The product was crystallized from dichloromethane to remove sodium chloride. The yield was 55% based on vanadium. Recrystallization from dichloromethane/toluene (1/1 v/v) gave pale purple crystals as a mixture of diamond-shaped and hexagonal plates. Anal. Calcd for $C_{52}H_{69}N_{14}B_2O_6V_2$ (III·2toluene): C, 56.4; H, 6.38; N, 18.8; V, 8.56. Found: C, 56.2; H, 6.4; N, 17.7; V, 8.0.

Physical Methods. Infrared spectra were obtained as Nujol mulls between cesium iodide plates using a Perkin-Elmer 1710 FT-IR instrument. Electronic absorption spectra were recorded in matched 1-cm quartz cells using a Shimadzu UV260 instrument. ESR spectra were obtained on a Varian E112 spectrometer system operating at either X- or Q-band frequency. Samples were contained in quartz tubes, and temperature control in the range 3.6–300 K was effected using an Oxford Instruments ESR9 continuous-flow cryostat at X-band frequency, with a Harwell DT temperature controller and VC flowmeter. At Q-band, samples were cooled to 150 K by conduction through the aluminum tuning rod using a narrow-necked dewar containing liquid dinitrogen. Double integration of the spectra was achieved using digitized data collected through a Biodata interface to an Apricot F2 microcomputer and an in-house integration program. Cyclic voltammograms were obtained using a Princeton AR Model 173 potentiostat and a Model 175 universal programmer with tetrabutylammonium tetrafluoroborate as supporting electrolyte with a platinum working electrode, a platinum auxiliary electrode, and a calomel reference electrode. Dichloromethane was used as solvent with ferrocene as an internal reference. Mass spectra were obtained using positive-ion FAB with a Kratos Concept 1S instrument. Elemental analyses were performed by the staff of the microanalytical laboratory of the Chemistry Department of the University of Manchester.

Table I. Summary of Crystallographic Data for [{HB(Me$_2$pz)$_3$}VOCl(Me$_2$pzH)] (I), [{HB(Me$_2$pz)$_3$}VO(benzoate)(Me$_2$pzH)] (II), and [{HB(Me$_2$pz)$_3$}VO(μ-malonate)VO(Me$_2$pzH){HB(Me$_2$pz)$_3$}] (III)

	I	II	III
empirical formula	$C_{24}H_{36}BN_{10}OClV$	$C_{29.8}H_{38.2}BN_8O_3V$	$C_{52}H_{69}B_2N_{14}O_6V_2$
fw	577.82	618.2	1109.7
space group	$P\bar{1}$ (No. 2)	$P\bar{3}$ (No. 147)	$P\bar{1}$ (No. 2)
unit cell dimens			
a/Å	9.986(3)	24.320(3)	13.859(4)
b/Å	10.898(3)		13.843(3)
c/Å	16.007(3)	9.233(1)	16.860(4)
α/deg	71.50(2)		76.07(2)
β/deg	79.86(2)		72.50(2)
γ/deg	65.70(2)		73.77(2)
V/Å^3	1503.2(7)	4730.2(12)	2918.3(13)
Z	2	6	2
T/K	294	294	294
d(calcd)/g cm^{-3}	1.277	1.302	1.266
min/max transm	0.6400/0.8804	0.5494/0.7502	0.6867/0.8931
R, R_w/%	5.42, 4.99	7.61, 9.38	8.42, 8.62

Collection and Analysis of X-ray Data. Crystals of the solvates of I–III were mounted in Lindemann capillaries containing the appropriate solvent; the capillaries were then flame-sealed, and measurements were taken on a Siemens R3m/v diffractometer. Mo Kα radiation (λ = 0.710 73 Å) was used and monochromated with a highly oriented graphite crystal. Preliminary data from a photographic setting scan of the diffractometer used 25 chosen reflections for accurate centering, initial choices of the unit cell constants, and an orientation matrix. Intensity data were then collected at room temperature. Crystal data and data collection parameters summarized in Table I and in the supplementary material. Semiempirical absorption corrections were used. The scattering factors were taken from ref 14, and the usual allowance was made for anomalous dispersion. II·0.4toluene and III·2toluene diffracted weakly.

Solution and Refinement of the Structures. Data were reduced and manipulated and the models refined using the Siemens SHELXTL PLUS package operating under VMS. Structures were solved by standard Patterson and direct methods and refined by full-matrix least-squares techniques. Parameters used in the solution and refinement of the structures are summarized in the supplementary material. Hydrogen atoms were treated using a riding model. Anisotropic thermal parameters and fixed isotropic hydrogen atom parameters are available as supplementary material. The final fractional atomic coordinates for the compounds are given in Tables II–IV, and selected distances and angles are given in Tables V–VII.

I·2MeCN. All non-hydrogen atoms were refined anisotropically. Structure solution and refinement proceeded straightforwardly.

II·0.4toluene. The small size of the crystal and the inherently weak diffraction led to the relatively high R_w value of ca. 9%. However the positions of all the non-hydrogen and non-solvent atoms were well defined. The disordered solvent was modeled by assigning the three largest peaks

(11) (a) Kime-Hunt, E.; Spartalian, K.; De Rusha, M.; Nunn, C. M.; Carrano, C. J. *Inorg. Chem.* **1989**, *28*, 4392. (b) Holmes, S.; Carrano, C. J. *Inorg. Chem.* **1991**, *30*, 1231.
(12) Kim, J.; Rees, D. C. *Science (Washington, D.C.)*, in press.
(13) (a) Trofimenko, S. *J. Am. Chem. Soc.* **1967**, *89*, 6288. (b) Bristow, S.; Collison, D.; McAvilley, S. C. M.; Clegg, W. *Polyhedron* **1989**, *8*, 87.
(14) *International Tables for X-ray Crystallography*; Kynoch Press: Birmingham, U.K., 1974.

Table II. Fractional Atomic Coordinates ($\times 10^4$) and Equivalent Isotropic Displacement Coefficients ($Å^2 \times 10^3$) for [{HB(Me$_2$pz)$_3$}VOCl(Me$_2$pzH)] (I)

	x	y	z	U(eq)[a]
V	786(1)	4122(1)	7463(1)	37(1)
Cl	−1339(2)	4138(2)	8408(1)	55(1)
O(1)	292(4)	5773(4)	7035(2)	51(2)
N(1)	−25(5)	3752(4)	6476(3)	40(2)
N(2)	805(5)	2666(4)	6105(3)	39(2)
C(1)	−1251(6)	4506(6)	6020(4)	44(3)
C(2)	−1217(7)	3889(6)	5376(4)	51(3)
C(3)	65(6)	2746(6)	5442(3)	43(3)
C(4)	−2423(6)	5768(6)	6229(4)	60(3)
C(5)	637(7)	1672(6)	4934(4)	63(4)
N(3)	2811(4)	3568(4)	6730(3)	36(2)
N(4)	3299(4)	2476(4)	6356(3)	37(2)
C(6)	3856(6)	4136(6)	6496(3)	41(3)
C(7)	4981(6)	3394(6)	6006(4)	49(3)
C(8)	4609(6)	2344(6)	5921(3)	43(3)
C(9)	3698(7)	5391(6)	6756(4)	62(3)
C(10)	5450(6)	1246(6)	5457(4)	63(3)
N(5)	1695(4)	1671(4)	8041(3)	38(2)
N(6)	2132(5)	909(4)	7430(3)	38(2)
C(11)	1622(6)	772(6)	8826(3)	44(3)
C(12)	1996(6)	−553(6)	8716(4)	49(3)
C(13)	2309(6)	−435(5)	7839(4)	45(3)
C(14)	1238(7)	1176(6)	9663(4)	62(3)
C(15)	2742(7)	−1522(6)	7347(4)	63(3)
B	2309(7)	1642(7)	6452(4)	37(3)
N(7)	1952(5)	4048(4)	8488(3)	40(2)
N(8)	3324(5)	3065(5)	8699(3)	46(2)
C(16)	1694(7)	4957(6)	8951(4)	49(3)
C(17)	2895(7)	4537(7)	9449(4)	64(4)
C(18)	3912(7)	3343(7)	9272(4)	56(3)
C(19)	298(7)	6223(6)	8886(4)	69(4)
C(20)	5398(7)	2423(8)	9605(5)	88(5)
C(21)	4119(8)	680(8)	1894(5)	76(4)
N(9)	4676(7)	−320(7)	1707(5)	94(4)
C(22)	3425(8)	1972(8)	2149(6)	112(5)
C(23)	8150(8)	1553(7)	7653(4)	82(4)
N(10)	8878(9)	−207(8)	6758(5)	127(6)
C(24)	8578(8)	552(8)	7154(5)	74(4)

[a] Equivalent isotropic U defined as one-third of the trace of the orthogonalized U_{ij} tensor.

in the final difference map to fractionally occupied carbon atom sites such that there is 0.4 toluene molecule per asymmetric unit as suggested by the elemental microanalytical data. The vanadium, the atoms of its first coordination sphere, and the entire benzoate ion were refined anisotropically.

III·2toluene. In the crystallographic determination, very few of the reflections measured were strong. Even before any were omitted, at least 50% were too weak to be counted as observed. Consequently, only the atoms in the coordination sphere of the vanadium were refined anisotropically. The toluene molecules of crystallization were modeled as regular hexagons with an extra carbon atom. The length of the bond to this extra carbon atom was unconstrained. The positions of the hydrogen atoms could be observed in difference maps, but these were fixed in idealized positions.

Results and Discussion

Syntheses. The complexes are formed by a series of ligand substitution reactions exclusively at the vanadium(IV) level, so that there are no overall redox reactions involved. The LVO^+ moiety is formed in a relatively low yield (20–30%) from [$VOCl_2$(MeCN)$_2$(H_2O)], despite many attempts to optimize this reaction. This and the nonquantitative conversion of LVOCl(Me$_2$pzH) to the carboxylate complexes suggest that the vanadyl unit sensitizes the B–N bond to cleavage. The neutral 3,5-dimethylpyrazole (Me$_2$pzH) molecule acting as a ligand in I is derived from KL, which was shown to be pure and free of Me$_2$pzH by elemental and spectroscopic analysis. Such low yields in reactions between vanadium and KL are also a feature of the work of Carrano et al.[11] In addition, a similar B–N bond cleavage reaction has been

Table III. Fractional Atomic Coordinates ($\times 10^4$) and Equivalent Isotropic Displacement Coefficients ($Å^2 \times 10^3$) for [{HB(Me$_2$pz)$_3$}VO(benzoate)(Me$_2$pzH)] (II)

	x	y	z	U(eq)[a]
V(1)	5967(1)	6804(1)	878(1)	31(1)
O(1)	6205(3)	6443(3)	1912(7)	45(3)
N(1)	5042(3)	6427(3)	1710(8)	38(4)
N(2)	4524(3)	6214(3)	805(7)	34(2)
C(1)	4818(4)	6322(4)	3071(10)	45(2)
C(2)	4150(4)	6043(4)	3025(10)	48(2)
C(3)	3986(4)	5978(4)	1613(9)	40(2)
C(4)	5258(5)	6493(5)	4315(11)	61(3)
C(5)	3342(4)	5705(5)	964(10)	53(2)
N(3)	5609(3)	7311(3)	−606(7)	34(3)
N(4)	5043(3)	6952(3)	−1297(7)	30(2)
C(6)	5874(4)	7900(4)	−1151(9)	38(2)
C(7)	5465(4)	7907(4)	−2223(10)	45(2)
C(8)	4957(4)	7318(4)	−2277(9)	37(2)
C(9)	6492(4)	8426(4)	−682(10)	52(2)
C(10)	4367(5)	7053(5)	−3222(11)	59(3)
N(5)	5552(3)	6063(3)	−646(8)	34(3)
N(6)	4969(3)	5891(3)	−1273(7)	31(2)
C(11)	5718(4)	5655(4)	−1160(10)	40(2)
C(12)	5277(4)	5241(4)	−2102(10)	46(2)
C(13)	4811(4)	5382(4)	−2178(9)	40(2)
C(14)	6346(4)	5708(4)	−728(11)	51(3)
C(15)	4201(5)	5079(5)	−3036(11)	61(3)
B(1)	4623(5)	6257(4)	−863(11)	36(2)
N(7)	6800(3)	7265(3)	−413(8)	41(4)
N(8)	7362(3)	7557(3)	321(9)	48(2)
C(16)	6958(5)	7339(5)	−1820(11)	49(2)
C(17)	7617(5)	7674(6)	−1944(14)	69(3)
C(18)	7845(5)	7810(5)	−627(11)	57(3)
C(19)	6487(5)	7109(5)	−3001(11)	59(3)
C(20)	8522(6)	8163(7)	−22(15)	96(4)
O(2)	6230(3)	7580(3)	2078(6)	42(3)
O(3)	7173(3)	7844(3)	3073(8)	66(4)
C(21)	6685(5)	7892(5)	2932(11)	48(5)
C(23)	6112(3)	8468(3)	3663(6)	59(6)
C(24)	6075	8934	4466	81(8)
C(25)	6548	9297	5469	98(10)
C(26)	7058	9194	5669	94(9)
C(27)	7095	8728	4866	68(6)
C(22)	6622	8365	3863	51(5)
C(30)	−539(1)	−513(1)	2853(1)	234(1)
C(32)	−617(1)	401(1)	6069(1)	298(1)
C(33)	0	0	7108(1)	173(1)

[a] Equivalent isotropic U defined as one-third of the trace of the orthogonalized U_{ij} tensor.

reported previously for rhenium–oxo complexes.[15] The production of II and III from I entails a salt precipitation reaction to displace the chloride ligand, either as a silver or a sodium salt. Addition of Me$_2$pzH to the reaction mixture in the preparation of I led to only a marginal increase in yields. The existence of these compounds is consistent with previous observations that the oxo complexes of the early d transition metals display a preference for the production of neutral complexes when ligated by hydrotris(3,5-dimethylpyrazolyl)borate.

Description of the Crystal and Molecular Structures. The crystallographic data are collected together for compounds I·2MeCN, II·0.4toluene, and III·2toluene in Table I. In each case, the ligand L functions in its typical tridentate mode with no unusual geometric features.[16] ORTEP diagrams showing the full atom-numbering scheme for each complex are given in Figures 1–3.

I·2MeCN and II·0.4toluene. These two monomeric complexes show the expected distorted octahedral geometry for the $\{LVO\}^+$ moiety with the nitrogen atom from a neutral 3,5-dimethylpyrazole molecule bound cis to the terminal oxo group and the sixth coordination position filled by either a chloride (I) or a benzoate oxygen (II) atom. There is the usual trans lengthening of the

(15) Backes-Dahmann, G.; Enemark, J. H. *Inorg. Chem.* **1987**, *26*, 3960.
(16) Trofimenko, S. *Prog. Inorg. Chem.* **1986**, *34*, 115.

Table IV. Fractional Atomic Coordinates (×10⁴) and Equivalent Isotropic Displacement Coefficients (Å² × 10³) for [{HB(Me₂pz)₃}VO(μ-malonate)VO(Me₂pzH){HB(Me₂pz)₃}] (III)

	x	y	z	U(eq)[a]		x	y	z	U(eq)[a]
V(1)	6461(2)	7098(2)	6628(2)	46(1)	C(22)	6396(12)	9749(12)	8977(9)	75(5)
O(1)	6545(7)	5928(7)	7041(6)	60(5)	C(23)	7767(13)	9380(12)	11539(9)	80(5)
N(1)	5771(9)	7063(8)	5666(8)	53(6)	N(9)	8669(9)	6478(8)	9811(7)	48(6)
N(2)	6199(9)	7372(8)	4838(7)	44(3)	N(10)	8942(9)	6681(9)	10469(7)	49(3)
C(4)	5044(13)	6555(12)	5732(10)	62(5)	C(24)	8522(11)	5506(12)	10033(9)	53(4)
C(5)	5049(12)	6569(11)	4898(10)	66(5)	C(25)	8698(12)	5095(12)	10844(10)	64(5)
C(6)	5728(11)	7068(11)	4365(9)	51(4)	C(26)	8933(12)	5843(12)	11094(10)	61(4)
C(7)	4418(14)	6104(13)	6534(10)	90(6)	C(27)	8202(12)	5034(12)	9490(9)	73(5)
C(8)	6029(13)	7282(13)	3444(10)	83(5)	C(28)	9201(14)	5811(13)	11910(10)	92(6)
N(3)	6414(9)	8775(8)	5912(7)	50(6)	N(11)	10084(9)	7743(8)	8868(7)	52(6)
N(4)	6625(8)	8931(8)	5040(7)	44(3)	N(12)	10075(10)	7873(8)	9651(8)	54(3)
C(9)	6076(11)	9708(12)	6117(9)	56(4)	C(29)	11012(13)	7824(11)	8333(10)	61(4)
C(10)	6091(11)	10445(12)	5397(9)	56(4)	C(30)	11612(14)	8000(12)	8793(11)	77(5)
C(11)	6407(11)	9957(11)	4733(9)	54(4)	C(31)	11034(14)	8015(12)	9574(11)	70(5)
C(12)	5805(12)	9869(11)	7003(9)	65(5)	C(32)	11303(13)	7721(12)	7430(9)	79(5)
C(13)	6574(13)	10357(13)	3800(10)	85(6)	C(33)	11272(15)	8274(15)	10319(11)	115(7)
N(5)	7896(9)	6845(8)	5712(7)	47(6)	B(2)	9182(14)	7724(13)	10393(11)	54(5)
N(6)	8013(9)	7335(8)	4885(7)	45(3)	N(13)	8754(9)	8796(8)	7673(6)	45(6)
C(14)	8855(12)	6267(11)	5767(9)	47(4)	N(14)	8677(8)	8607(8)	6928(7)	45(3)
C(15)	9558(12)	6406(11)	4982(9)	58(4)	C(34)	9056(11)	9660(12)	7462(9)	52(4)
C(16)	9001(12)	7061(11)	4445(9)	51(4)	C(35)	9170(11)	10035(11)	6614(9)	55(4)
C(17)	9028(12)	5601(12)	6567(9)	70(5)	C(36)	8906(11)	9345(10)	6290(9)	45(4)
C(18)	9370(14)	7490(13)	3542(10)	94(6)	C(37)	9254(12)	10133(11)	8095(9)	72(5)
B(1)	7008(14)	8001(13)	4602(12)	56(5)	C(38)	8888(12)	9311(12)	5409(9)	70(5)
O(3)	5138(7)	7723(7)	7319(7)	56(5)	C(40)	4482(13)	7380(16)	891(10)	135(8)
O(4)	7183(7)	7432(7)	7395(6)	44(5)	C(41)	5336	7629	1001	157(10)
C(1)	4944(13)	7695(13)	8111(13)	63(9)	C(42)	6120	6860	1275	171(10)
C(2)	5755(11)	7111(12)	8605(9)	59(8)	C(43)	6050	5841	1439	182(11)
C(3)	6817(11)	7343(10)	8195(10)	43(7)	C(44)	5195	5592	1329	192(12)
O(5)	4113(9)	8127(10)	8528(7)	87(7)	C(45)	4411	6362	1055	258(18)
O(6)	7291(7)	7454(6)	8678(5)	46(3)	C(46)	3692(41)	6123(37)	855(29)	338(24)
V(2)	8749(2)	7499(2)	8674(2)	41(1)	C(50)	2690(12)	5697(9)	4381(13)	94(6)
O(2)	9360(7)	6700(7)	8052(6)	53(5)	C(51)	2970	6359	3628	193(12)
N(7)	7878(8)	8637(8)	9561(7)	47(6)	C(52)	2827	7396	3633	218(14)
N(8)	8219(9)	8565(8)	10262(7)	47(3)	C(53)	2403	7771	4392	142(9)
C(19)	7016(12)	9405(12)	9625(9)	55(4)	C(54)	2123	7108	5145	124(8)
C(20)	6839(12)	9836(11)	10332(9)	58(4)	C(55)	2267	6071	5139	179(12)
C(21)	7590(11)	9287(11)	10740(9)	52(4)	C(56)	2077(26)	5478(26)	5710(21)	212(13)

[a] Equivalent isotropic U defined as one-third of the trace of the orthogonalized U_{ij} tensor.

Table V. Selected Bond Lengths and Angles for [{HB(Me₂pz)₃}VOCl(Me₂pzH)] (I)

Bond Lengths (Å)			
V–Cl	2.377(2)	V–O(1)	1.599(4)
V–N(1)	2.107(6)	V–N(3)	2.107(4)
V–N(5)	2.355(4)	V–N(7)	2.136(5)
Bond Angles (deg)			
Cl–V–O(1)	98.3(1)	Cl–V–N(1)	91.8(1)
O(1)–V–N(1)	95.8(2)	Cl–V–N(3)	165.8(1)
O(1)–V–N(3)	95.8(2)	N(1)–V–N(3)	85.1(2)
Cl–V–N(5)	86.0(1)	O(1)–V–N(5)	175.6(2)
N(1)–V–N(5)	84.7(2)	N(3)–V–N(5)	79.9(1)
Cl–V–N(7)	92.7(1)	O(1)–V–N(7)	95.0(2)
N(1)–V–N(7)	167.6(2)	N(3)–V–N(7)	87.7(2)
N(5)–V–N(7)	84.1(2)	V–N(1)–N(2)	121.6(3)
V–N(1)–C(1)	131.2(4)	V–N(3)–C(6)	132.0(4)
V–N(3)–N(4)	122.1(4)	V–N(5)–N(6)	115.9(3)
V–N(5)–C(11)	136.0(4)	V–N(7)–N(8)	122.7(4)
V–N(7)–C(16)	131.6(3)		

Table VI. Selected Bond Lengths and Angles for [{HB(Me₂pz)₃}VO(benzoate)(Me₂pzH)] (II)

Bond Lengths (Å)			
V(1)–O(1)	1.590(8)	V(1)–N(1)	2.106(7)
V(1)–N(3)	2.285(8)	V(1)–N(5)	2.105(7)
V(1)–N(7)	2.122(7)	V(1)–O(2)	1.996(6)
Bond Angles (deg)			
O(1)–V(1)–N(1)	98.3(3)	O(1)–V(1)–N(3)	179.1(2)
N(1)–V(1)–N(3)	80.9(3)	O(1)–V(1)–N(5)	94.5(3)
N(1)–V(1)–N(5)	85.4(3)	N(3)–V(1)–N(5)	85.0(3)
O(1)–V(1)–N(7)	96.5(3)	N(1)–V(1)–N(7)	164.7(3)
N(3)–V(1)–N(7)	84.2(3)	N(5)–V(1)–N(7)	90.0(3)
O(1)–V(1)–O(2)	98.9(3)	N(1)–V(1)–O(2)	88.7(3)
N(3)–V(1)–O(2)	81.5(3)	N(5)–V(1)–O(2)	166.0(3)
N(7)–V(1)–O(2)	92.4(3)	V(1)–N(1)–N(2)	121.3(5)
V(1)–N(1)–C(1)	131.9(6)	V(1)–N(3)–C(6)	133.8(6)
V(1)–N(3)–N(4)	118.1(5)	V(1)–N(5)–N(6)	121.1(6)
V(1)–N(5)–C(11)	133.1(6)	V(1)–N(7)–C(16)	138.5(6)
V(1)–N(7)–N(8)	116.0(5)	V(1)–O(2)–C(21)	133.5(9)

vanadium–nitrogen bond caused by the terminal oxo group. Figure 4 shows line drawings of the coordination environment and framework of all three complexes and reveals the presence of intramolecular hydrogen bonding in complexes II and III. A comparison of I and II in Figure 4 shows that Me₂pzH, the neutral pyrazole molecule, is rotated about the V(1)–N(7) bond between these two structures (and the V(2)–N(13) bond in III), such that a hydrogen bond of 1.902 Å is formed between H(8) and O(3) in II (and H(14a) and O(4) in III of 2.045 Å). In this manner, the N–N bond of the ligating Me₂pzH molecule lies on the same side of the complex as the carboxylate oxygen atoms (O(2) and O(3) in II and O(4) and O(6) in III) but is rotated away when the sixth ligand is chloride. A consideration of the unit cell packing diagram for I does not show any additional reason for such a rotation. Selected bond lengths and angles for I and II are given in Tables V and VI, respectively. This terminal unidentate mode of bonding by benzoate to vanadium(IV) is in contrast to the bridging mode found[17] in the distorted, oxo-centered, trinuclear cluster $[V_3(O)_3(\text{tetrahydrofuran})(C_6H_5CO_2)_6]$.

III·2toluene. The complex forms as an asymmetric dimer from two LVO^+ fragments (see Figures 3 and 4). The coordination sphere of V(1) is completed by a six-membered chelate

(17) Cotton, F. A.; Lewis, G. E.; Mott, G. N. *Inorg. Chem.* **1982**, *21*, 3127.

Table VII. Selected Bond Lengths and Angles for [{HB(Me$_2$pz)$_3$}VO(μ-malonate)VO(Me$_2$pzH){HB(Me$_2$pz)$_3$}] (III)

Bond Lengths (Å)

V(1)–O(1)	1.587(9)	V(1)–N(1)	2.130(15)
V(1)–N(3)	2.338(11)	V(1)–N(5)	2.118(10)
V(1)–O(3)	1.945(9)	V(1)–O(4)	2.053(12)
V(2)–O(2)	1.592(9)	O(6)–V(2)	2.037(11)
V(2)–N(9)	2.084(10)	V(2)–N(7)	2.273(11)
V(2)–N(13)	2.148(10)	V(2)–N(11)	2.100(15)

Bond Angles (deg)

O(1)–V(1)–N(1)	96.2(6)	O(1)–V(1)–N(3)	175.2(5)
N(1)–V(1)–N(3)	81.1(5)	O(1)–V(1)–N(5)	94.8(4)
N(1)–V(1)–N(5)	86.0(5)	N(3)–V(1)–N(5)	81.1(4)
O(1)–V(1)–O(3)	101.2(4)	N(1)–V(1)–O(3)	92.4(5)
N(3)–V(1)–O(3)	82.9(4)	N(5)–V(1)–O(3)	164.0(4)
O(1)–V(1)–O(4)	96.0(5)	N(1)–V(1)–O(4)	167.4(4)
N(3)–V(1)–O(4)	86.6(4)	N(5)–V(1)–O(4)	89.8(5)
O(3)–V(1)–O(4)	88.4(5)	V(1)–N(1)–N(2)	121.7(10)
V(1)–N(1)–C(4)	127.6(10)	V(1)–N(3)–N(4)	117.2(9)
V(1)–N(3)–C(9)	136.5(9)	V(1)–N(5)–N(6)	122.2(8)
V(1)–N(5)–C(14)	132.0(9)	V(1)–O(3)–C(1)	124.6(10)
V(1)–O(4)–C(3)	122.2(10)	O(6)–V(2)–O(2)	96.9(5)
O(6)–V(2)–N(7)	83.1(4)	O(2)–V(2)–N(7)	180.0(6)
O(6)–V(2)–N(9)	91.0(4)	O(2)–V(2)–N(9)	98.2(4)
N(7)–V(2)–N(9)	81.8(4)	O(6)–V(2)–N(11)	167.7(4)
O(2)–V(2)–N(11)	95.4(5)	N(7)–V(2)–N(11)	84.6(5)
N(9)–V(2)–N(11)	86.0(5)	O(6)–V(2)–N(13)	91.3(4)
O(2)–V(2)–N(13)	93.8(4)	N(7)–V(2)–N(13)	86.3(4)
N(9)–V(2)–N(13)	167.5(5)	N(11)–V(2)–N(13)	89.2(5)
V(2)–N(7)–N(8)	118.3(7)	V(2)–N(7)–C(19)	136.7(11)
V(2)–N(9)–N(10)	120.6(9)	V(2)–N(9)–C(24)	131.6(11)
V(2)–N(11)–C(29)	131.2(12)	V(2)–N(11)–N(12)	119.5(8)
V(2)–N(13)–C(34)	138.5(11)	V(2)–N(13)–N(14)	114.1(8)

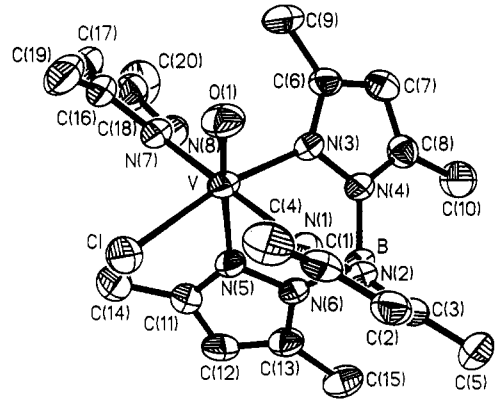

Figure 1. Structure of [{HB(Me$_2$pz)$_3$}VOCl(Me$_2$pzH)] (I), shown by an ORTEP diagram with 50% probability thermal ellipsoids and the atom-numbering scheme.

ring from the malonate dianion. One of the remaining nonligating oxygen atoms of the carboxylato group then forms a bridge to V(2), with six-coordination for this vanadium atom being achieved via a nitrogen atom of a neutral Me$_2$pzH molecule. This bridging mode for the malonate dianion has been reported previously[18a] for a polymeric manganese(III) complex but has not been observed in a discrete dimeric complex.[18b] According to the principles of Glusker et al.,[7] this dicarboxylate acts as (i) a single monodentate carboxylate (V(1)–O(3)), (ii) a bridging dicarboxylate (V(1)–O(4)–C(3)–O(6)–V(2)), and (iii) a six-membered chelating dicarboxylate (V(1)–O(3)–C(1)–C(2)–C(3)–O(4)). Examples of (i) (this work), (ii),[18a] and (iii)[18b] have been reported for separate complexes. One which contains *all* three elements in a discrete complex is not known. The coordination geometry about the vanadium ion is essentially similar for both LV(1)O(O,O) and LV(2)O(O,N) environments with a short, terminal V=O distance

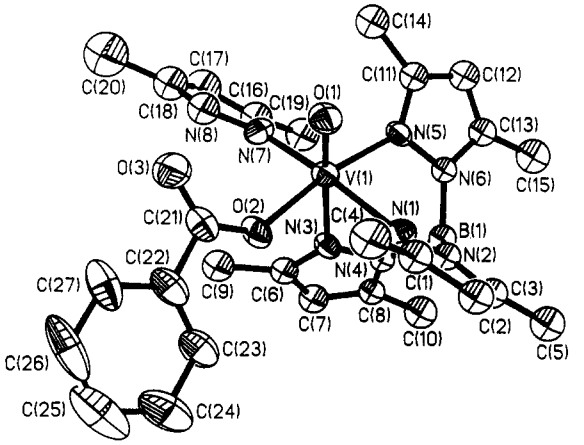

Figure 2. Structure of [{HB(Me$_2$pz)$_3$}VO(benzoate)(Me$_2$pzH)] (II), shown by an ORTEP diagram with 50% probability thermal ellipsoids and the atom-numbering scheme.

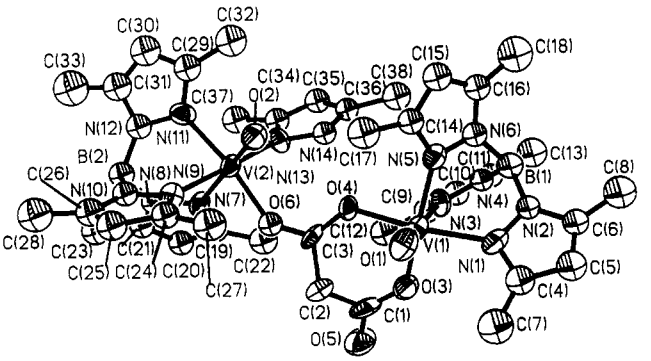

Figure 3. Structure of [{HB(Me$_2$pz)$_3$}VO(μ-malonate)VO(Me$_2$pzH)-{HB(Me$_2$pz)$_3$}] (III), shown by an ORTEP diagram with 50% probability thermal ellipsoids and the atom-numbering scheme.

of ca. 1.59 Å. This leads to the expected trans lengthening of V—N (derived from one of the pyrazolyl rings of L). This lengthening is slightly less pronounced for V(2) than for V(1). The pyrazolyborate units show the expected geometric parameters for a facial bonding mode. A monomeric, bis(malonato) complex of oxovanadium(IV) has had its crystal and molecular structure reported previously[19] and shows the six-membered ring chelate structure found for V(1) in III. Selected bond lengths and angles are given in Table VII.

Physical and Spectroscopic Properties. Selected physical and spectroscopic properties of complexes I–III are collected in Table VIII. The Nujol mull infrared spectra serve as a good fingerprint with characteristic frequencies for ν(V=O)$_{str}$ and ν(B—H)$_{str}$ around 970 and 2500 cm^{-1}, respectively. The identification of these two stretching frequencies is distinct for each of the three compounds studied, but the asymmetric nature of the oxovanadium(IV) sites in III is *not* apparent in the infrared spectrum. However, the two types of 3,5-dimethylpyrazole ring systems can be identified in the ν(C=N) region (ca. 1530–1600 cm^{-1}), where for complexes I and II there are two peaks in ca. 3:1 ratio of intensity. The higher frequency peak is assigned to the neutral pyrazole ligand from a consideration of the relative intensities of the peaks. For III two peaks are also observed in the ν(C=N) region. In addition, bands attributable to ligated carboxylate are apparent in the region 1600–1700 cm^{-1} for complexes II and III. ν(C≡N) vibrations from the methyl cyanide solvate are seen at 2270 and 2300 cm^{-1} for I and are absent for II and III.

The compounds are also amenable to characterization by positive-ion FAB mass spectrometry as we have previously observed[20] for other neutral compounds containing the LMO^{n+}

(18) (a) Lis, T.; Matuszewski, J. *J. Chem. Soc., Dalton Trans.* **1980**, 996. (b) Shibahara, T.; Kuroya, H.; Matsumoto, K.; Ooi, S. *Inorg. Chim. Acta* **1981**, *54*, L75.

(19) Pajunen, A.; Pajunen, S. *Acta Crystallogr., Sect. B* **1980**, *36*, 2425.

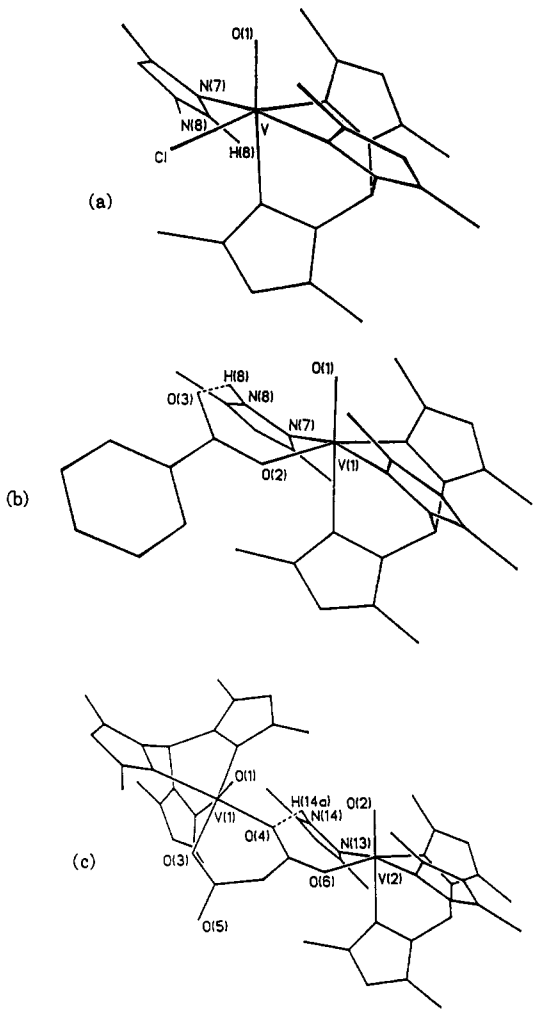

Figure 4. Line drawings of (a) [{HB(Me2pz)3}VOCl(Me2pzH)] (I), (b) [{HB(Me2pz)3]VO(benzoate)(Me2pzH)] (II), and (c) [{HB(Me2pz)3}-VO(μ-malonate)VO(Me2pzH){HB(Me2pz)3}] (III), showing the stereochemistry at the vanadium atom and intramolecular hydrogen-bonding interactions.

moiety. For all the complexes, a peak corresponding to the parent ion is readily seen, and in each case, the LVO fragment is clearly present. The electronic absorption spectra of I–III recorded in dichloromethane solution show two bands of low extinction coefficient in the visible region consistent with their assignment as d–d transitions. The lower energy band at ca. 760 nm (13×10^3 cm^{-1}) is nearly constant in position and is twice as intense as the second band which is at 598 nm (16.7×10^3 cm^{-1}) for I and around 556 nm (17.98×10^3 cm^{-1}) for II and III. The extinction coefficients of the bands for III are significantly higher than those for I or II. These values may be compared with those of the series[21] [LVO(β-diketonate)], where the range of values for three d–d transitions are $(13.05–13.15) \times 10^3$, $(16.9–17.6) \times 10^3$, and $(20.83–24.22) \times 10^3$ cm^{-1}. In the new complexes reported herein, any d–d transition occurring at $>21 \times 10^3$ cm^{-1} would be obscured by the charge-transfer (CT) tail from the UV region of the spectrum. Such CT processes therefore arise from carboxylate and Me2pzH to metal transfer, since chlorine to metal transfer occurs at higher energy.[22]

Cyclic voltammograms of the three complexes (see Figure 5) in dichloromethane solution with tetrabutylammonium tetrafluoroborate as supporting electrolyte show a Nernstian, reversible one-electron oxidation process for the monomeric complexes at high (200 mV s^{-1}) scan rate, which becomes less reversible as the scan rate is slowed. The oxidation of II occurs at a potential ca. 200 mV less than that for I, which is consistent with the greater π-donor ability of the carboxylate ligand compared to that of chloride. Such a trend has also been identified by Holmes and Carrano[11b] for a series of [LVO(aryloxide)$_2$] complexes. These authors reported that this view of the π-bonding was mirrored in the values obtained for chemical shifts in ^{51}V NMR spectra. These data may also be compared[21] with those for the series [LVO(β-diketonate)], where $E(V^V/V^{IV})$ lies in the range 1.164–1.399 V vs SCE. Complex III does not show such simple electrochemical activity, undergoing an initial oxidation process at fast scan rates followed by a secondary process. The first couple can be tentatively assigned to electron transfer at V(2), by comparison with the characteristics of the oxidation of II, following the arguments above. The confirmation of the existence of a daughter product (estimated values: $E_{1/2} \approx 0.92$ V, $\Delta E_p \approx 60$ mV, $I_p^C/I_p^A \approx 0.8$) from the electrochemical oxidation of III and its characteristics were demonstrated as follows. Repeatedly scanning from 0.0 to +1.5 V resulted in an increase in the amplitude of both the reverse and forward peaks for the daughter product and a decrease in those of the parent. Decreasing the temperature of measurement resulted in an increase in the ratio I_p^C/I_p^A for the parent, from ca. 0.01 at 17.5 °C to 0.2 at −20 °C. Holding the applied potential at +1.5 V and waiting for time t resulted in a decrease in the current ratio of the parent as the wait time increased for scans between +1.5 and +0.6 V. In addition, the amplitude of the features corresponding to the daughter were seen to increase as t increased. Finally, scanning the applied voltage from 0.0 to +0.6 V did not produce any features in the cyclic voltammogram. Therefore we assign the daughter product as the result of chemical decomposition of the oxidized (parent) product of III. By comparison with ferrocene, recorded under the same conditions, all the primary electrochemical processes for the three complexes are assigned to one-electron events.

ESR and Magnetic Properties. The fluid-solution ESR spectra of complexes I–III in dichloromethane/toluene (1/1 v/v) are shown in Figure 6 for the data collected at X-band frequency and are entirely consistent with similar data collected at Q-band frequency. I and II each show the expected 8-line pattern of a monomeric species (^{51}V, $I = 7/2$, 99.96% abundant), with g_{iso} and A_{iso} values typical of oxovanadium(IV) complexes containing Cl$^-$ and O- and N-donor ligands in a distorted octahedral environment. Complex III shows a 15-line pattern as expected for a dimer; the spectrum does not change with time (ca. 24 h) and thus indicates that the dimeric structure found in the solid state persists in solution.

In frozen solution (X-band 77 K, Q-band 150 K) the ESR spectra of I and II appear axial, and spectral simulations on that basis give a good fit by eye, as seen in Figure 7. The parameters, in the caption to Figure 7, are as expected for oxovanadium(IV) complexes bound by Cl$^-$ and N- and O-donor groups. Complex III has a much more complicated frozen-glass spectrum which is of similar form at both frequencies. This similarity suggests that there is minimal zero-field splitting in the spin-Hamiltonian description of III. In contrast and as expected, the ESR spectra of powdered, polycrystalline samples of the solvates I, II, and III·2toluene each show a single, unstructured line at Q-band frequency, of 255-, 360-, and 350-G peak–peak line widths, respectively. Thus the spectra in solution afford a means of measuring *intra*molecular exchange.

In order to investigate the nature of the magnetic interaction between the metal centers in III, the intensities of the *total* ESR spectra of both II and III under nonsaturating conditions were double-integrated as a function of temperature in the range 80–3.6 K; see Figure 8. Complex II, the monomer, shows a gradual

(20) Cleland, W. E., Jr.; Barnhart, K. M.; Yamanouchi, K.; Collison, D.; Mabbs, F. E.; Ortega, R. B.; Enemark, J. H. *Inorg. Chem.* **1987**, *26*, 1017.
(21) Beddoes, R. L.; Collison, D.; Mabbs, F. E.; Passand, M. A. *Polyhedron* **1990**, *20*, 2483.
(22) Collison, D.; Gahan, B.; Garner, C. D.; Mabbs, F. E. *J. Chem. Soc., Dalton Trans.* **1980**, 667.

Table VIII. Selected Physical and Spectroscopic Properties of [{HB(Me$_2$pz)$_3$}VOCl(Me$_2$pzH)] (I), [{HB(Me$_2$pz)$_3$}VO(benzoate)(Me$_2$pzH)] (II), and [{HB(Me$_2$pz)$_3$}VO(μ-malonate)VO(Me$_2$pzH){HB(Me$_2$pz)$_3$}] (III)

complex	infrared ν/cm^{-1}	electronic absorption λ/nm (ϵ/dm^{-3} M^{-1})	cyclic voltammetry $E_{1/2}$/V vs SCE	mass spectra m/e (assignt)	ESR[a] g_{iso}	ESR[a] $-A_{iso}$/G
I	971 (V=O)	762 (54)	1.36	494 (M)	1.970	100
	2535 (B—H)	598 (21)		459 (M – Cl)		
	1574 (C=N (pzH))			363 (LVO)		
	1542 (C=N (pz))					
II	965 (V=O)	766 (17)	1.15	581 (M)	1.971	101.2
	2510 (B—H)	557 (9)		485 (M – pzH)		
	1595 (C=N (pzH))			364 (LVO)		
	1563 (C=N (pz))					
	1601 (C=O)					
III	970 (V=O)	764 (129)	0.92, 1.27	1193 (M)	1.974	50.5
	2520 (B—H)	555 (53)		364 (LVO)		
	1561 (C=N)					
	1539 (C=N)					
	1662 (C=O)					

[a] Estimated errors in the ESR parameters: g, ±0.002; A, ±1.0 G.

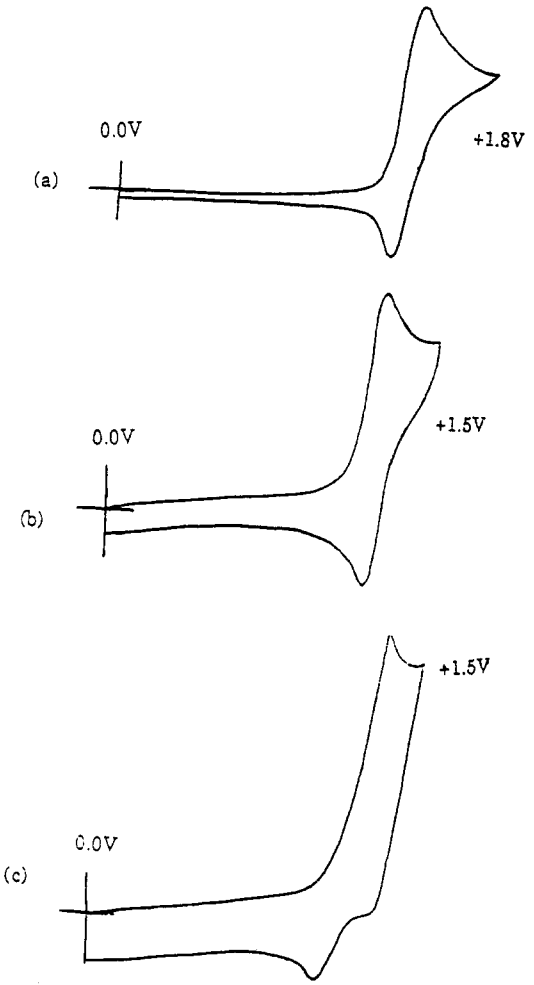

Figure 5. Cyclic voltammograms of (a) [{HB(Me$_2$pz)$_3$}VOCl(Me$_2$pzH)] (I), (b) [{HB(Me$_2$pz)$_3$}VO(benzoate)(Me$_2$pzH)] (II), and (c) [{HB(Me$_2$pz)$_3$}VO(μ-malonate)VO(Me$_2$pzH){HB(Me$_2$pz)$_3$}] (III), in dichloromethane. Peak separations (at –20 °C), ΔE and I_p^A/I_p^C: (I) 126 mV, 1.12; (II) 94 mV, 1.13; (III) 86 mV, 0.2. For ferrocene under the same conditions $E_{1/2}$ = 0.430 V, ΔE = 75 mV, and I_p^A/I_p^C = 1.05.

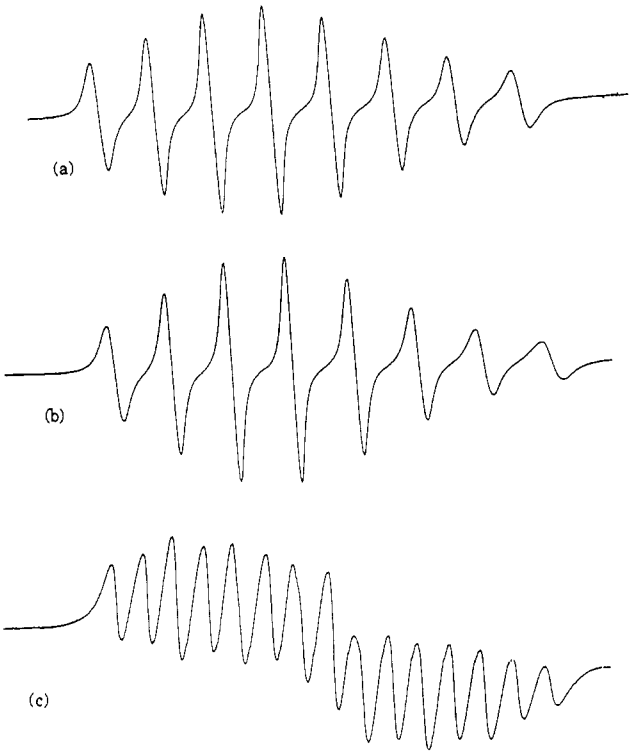

Figure 6. Fluid-solution ESR spectra of (a) [{HB(Me$_2$pz)$_3$}VOCl(Me$_2$pzH)] (I), (b) [{HB(Me$_2$pz)$_3$}VO(benzoate)(Me$_2$pzH)] (II), and (c) [{HB(Me$_2$pz)$_3$}VO(μ-malonate)VO(Me$_2$pzH){HB(Me$_2$pz)$_3$}] (III), in dichloromethane at X-band frequency. Scan range: 1000 G.

rise in integrated intensity from 80 to 20 K followed by a rapid rise down to 3.6 K. This curve follows the form expected of the varaition of magnetic susceptibility with temperature for an isolated, monomeric paramagnet. Complex III, the dimer, shows a more rapid rise in the higher temperature region, but below 15 K the rise is less rapid than that observed for II and at low temperature the spectral intensity begins to decrease. This behavior is consistent with an antiferromagnetic coupling between the vanadium ions in the dimer, which is estimated to be ca. 3 cm^{-1}, using the equations developed by Figgis.[23]

Conclusions

The LVO$^+$ moiety can be stabilized by the uninegative ligands chloride and carboxylate to produce neutral, six-coordinate complexes. The oxovanadium(IV) unit appears to sensitize the tris(3,5-dimethylpyrazolyl)hydroborate anion to B–N cleavage, as shown by the occurrence of the neutral 3,5-dimethylpyrazole molecule acting as a ligand in these complexes. The dicarboxylate ion malonate forms a novel bridge between the vanadium(IV) ions in complex III and transmits a weak antiferromagnetic coupling interaction. The synthesis of these carboxylato complexes should enable the nature of the bridge between metal centers to be further modified in this class of compound and thus vary

(23) (a) Kambé, K. *J. Phys. Soc. Jpn.* **1950**, *5*, 48. (b) Figgis, B. N.; Martin, R. L. *J. Chem. Soc.* **1956**, 3837. (c) Bleaney, B.; Bowers, K. D. *Proc. R. Soc. London* **1952**, *A214*, 451.

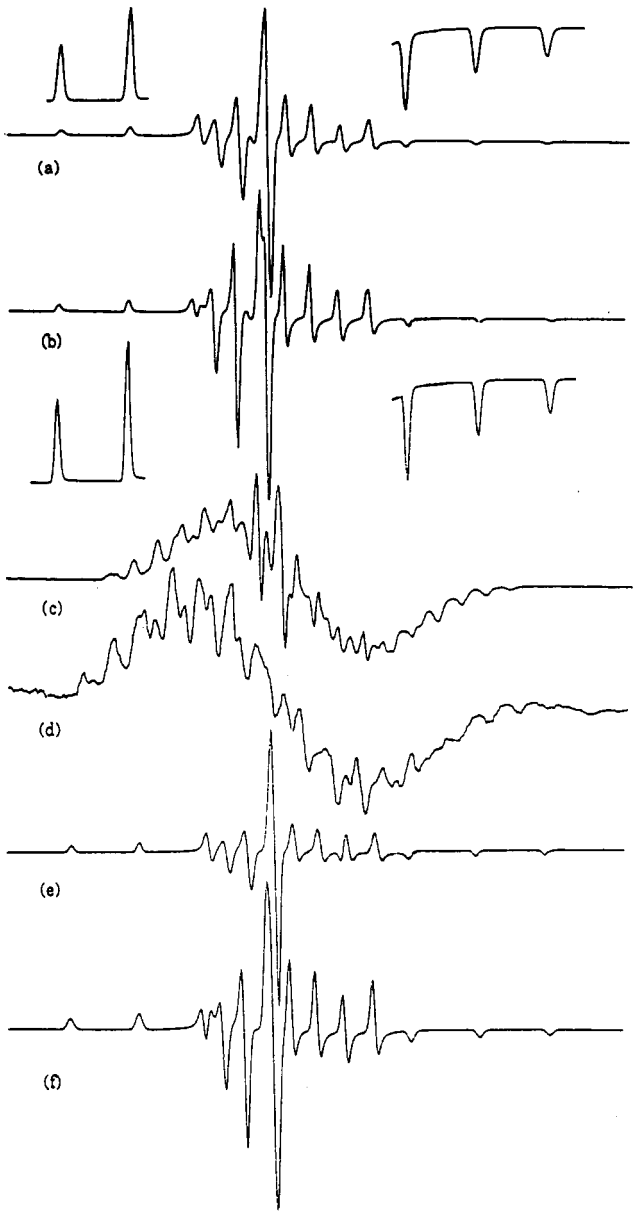

Figure 7. Frozen-solution ESR spectra of (a) [{HB(Me$_2$pz)$_3$}VOCl(Me$_2$pzH)] (I), (b) [{HB(Me$_2$pz)$_3$}VO(benzoate)(Me$_2$pzH)] (II), (c) [{HB(Me$_2$pz)$_3$}VO(μ-malonate)VO(Me$_2$pzH){HB(Me$_2$pz)}] (III), in dichloromethane/toluene at X-band frequency (77 K), and (d) [{HB(Me$_2$pz)$_3$}VO(μ-malonate)VO(Me$_2$pzH){HB(Me$_2$pz)}] (III), at Q-band frequency (150 K). Traces e and f are simulations of spectra a and b, respectively. Simulation parameters: (e) (I) $g_1 = 1.950$, $g_2 = g_3 = 1.981$, $A_1 = -178.0$ G, $A_2 = A_3 = -63.0$ G, $\Delta B_1 = 16$ G, $\Delta B_2 = \Delta B_3 = 13.6$ G; (f) (II) $g_1 = 1.955$, $g_2 = g_3 = 1.978$, $A_1 = -176.0$ G, $A_2 = A_3 = -62.5$ G, $\Delta B_1 = 12.0$ G, $\Delta B_2 = \Delta B_3 = 16.0$ G. All scan ranges are 1600 G. In the simulations, complexes I and II are assumed to be electronically axial and to have Gaussian line shapes. Estimated errors: g, ±0.002; A, ±1.0 G. Spectra a and b show expansions of the "parallel" hyperfine features.

the extent and magnitude of magnetic couplings. The novel

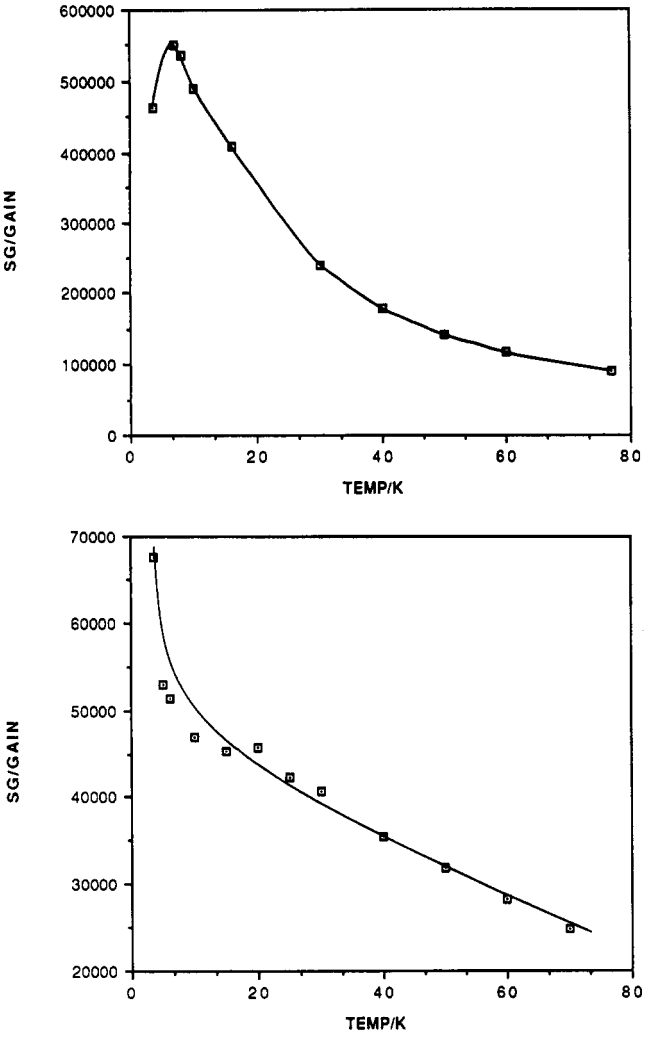

Figure 8. Temperature variation of the double-integrated intensity, under nonsaturating conditions for (top) [{HB(Me$_2$pz)$_3$}VO(benzoate)(Me$_2$pzH)] (II) and (bottom) [{HB(Me$_2$pz)$_3$}VO(μ-malonate)VO(Me$_2$pzH){HB(Me$_2$pz)$_3$}] (III), in dichloromethane/toluene at X-band frequency. The units on the ordinate are arbitrary values of the relative signal intensity divided by the spectrometer gain.

complexes reported herein are potential precursors to analogous carboxylato complexes of vanadium(V) which may form models for the active site of the vanadium-containing bromoperoxidases.

Acknowledgment. We thank The Royal Society (D.C. for a research fellowship), the SERC, U.K. (S.S.T. for a quota studentship), and the University of Manchester (D.R.E. for a postgraduate award) for financial support and Dr. K. J. Taylor for helpful discussions about the electrochemistry. We also thank a referee for drawing our attention to the cleavage reaction in ref 15.

Supplementary Material Available: Listings of structure determination details and thermal parameters and more extensive compilations of selected bond lengths and angles (14 pages). Ordering information is given on any current masthead page.